Vol. 39, No. 3 (2017) 364-377, DOI: 10.24874/ti.2017.39.03.12

Tribology in Industry

www.tribology.fink.rs

RESEARCH

Assessment of Tribological performance of Coconut Shell Ash Particle Reinforced Al-Si-Fe Composites using Grey-Fuzzy Approach

R.S.S. Raju[a], G.S. Rao[b]

[a] *Faculty of Mechanical Engineering, Gandhi Institute of Engineering and Technology, Gunupur, Odisha, India,*
[b] *Faculty of Mechanical Engineering, RVR & JC College of Engineering, Guntur, Andhra Pradesh, India.*

Keywords:

Coconut Shell Ash
Mechanical Properties
Metallography
Wear and Wear rate
Coefficient of friction
Grey relational grade
Grey-Fuzzy analysis

Corresponding author:

Siva Sankara Raju
Faculty of Mechanical Engineering, Gandhi Institute of Engineering and Technology, Gunupur, Odisha, India.
E-mail: sivaraju80@gmail.com

A B S T R A C T

The paper investigates optimization of wear behaviour of coconut shell ash (CSA) reinforced aluminium composites using pin-on-disc setup. The experiments were carried out with three process parameters: Load, percentage (%) of CSA and sliding distance. Three adequate responses: wear (μm), wear rate (mm^3/m) and coefficient of friction were considered. In this study, a hybrid approach (i.e. Grey-Fuzzy) has been applied to optimizing the several responses. The fuzzy logic concept has been used for handling the uncertainty in the decision-making process. Analysis of variance (ANOVA) discloses that the highest influencing parameter was load, followed by sliding distance and % of CSAp to the overall tribological performance.

1. INTRODUCTION

Aluminium metal matrix composites (AMC) have been widely utilised in transport, structure and well-designed applications of defence, aerospace, and sports due to the extensive property of intrinsic and extrinsic effect of ceramic reinforcement with physical, tribological and thermo-mechanical properties [1-4]. Generally, composites have been prepared with the addition of two important materials such as reinforcement and matrix. Aluminium and its alloys have attracted most attention as base metal in metal matrix composites. Therefore, AMCs can be prepared by the utilization of various ceramics such as SiC, Al_2O_3, TiO_2, graphite, mica, talc and boric acid, etc., and agro wastes such as fly ash, red mud, colliery shale, rice husk, shell char, bagasse, and breadfruit seed. However, there is a critical issue in preparation of the composite with respect to fabrication, processing, and characterization [1,5,6].

In this work, coconut shell ash was used as a reinforcement material. The coconut shell is an agro waste, easily available at low cost and can be processed to obtain CSA for the preparation of AMCs. The coconut shell has high lignin, which

supports weather resistance, improves corrosion resistance and increases the strength of the material [6]. Due to its exceptional orientation of structure and low ash content, coconut shell is preferable to making the activated carbon black [7].

The literature has shown that, wear rate and wear resistance are mostly influenced by the load, wt.% of reinforcement, sliding distance, sliding velocity and contact surface [8,9]. Sahin [8] optimized tribological performance of Al-SiC-MMCs using Taguchi approach. The size of particles was the main influencing parameter in wear mechanism, followed by the percentage of reinforcement. However, the sliding distance may not be significant on overall wear performance. Kok and Ozdin [9] investigated the wear mechanism of the Al-2024/Al_2O_3 composite and reported that wear resistance was increased by increasing reinforced particle size, percentage of volume and decreases with increase of sliding distance, and load. Baradeswaran et al. [10] explored the wear resistance of HMC reinforced with B_4C (10 wt.%) and Gr (5 wt.%) using response surface methodology. They observed that Mechanical Mixed Layer (MML) formed between tribo faces of composite was significantly influencing to wear properties of the composite.

Rao et al. [11] considered wear behaviour of AA2024 reinforced with fly ash particles, which results in higher resistance of composite than that of the base alloy at lower loads. The wear rises with increasing the load and sliding distance due to dislocations and fractured particles in the matrix of the composite. Siva et al. [12] inspected the mechanical properties, abrasion and frictional performance of Al-colliery shale (CS) and Al-Al_2O_3 composites under forged condition by using pin-on–disc set up. They reported that Al-colliery shale exhibited better mechanical properties like ductility, toughness, stiffness, tensile strength and percentage elongation than Al-Al_2O_3. The wear behaviour in the forged condition of Al-CS had superior characteristic than Al-Al_2O_3 and base matrix. Aku et al. [13] evaluated microstructure, hardness and density of coconut shell ash composites having 3-15 wt.%. They found that by increasing the wt.% of reinforcement, density decreased and hardness values increased.

Rajesh et al. [14] evaluated the dry sliding wear behaviour of SiC reinforced with aluminium using Grey –Taguchi approach. The authors reported that sliding velocity was the main influencing factor than wt.% of reinforcement, sliding distance and contact stress.

Moreover, statistical approaches such as Taguchi method [15–17], Response Surface Methodology [10,18], Grey Relational Analysis (GRA) [14,19–21]; soft computing techniques (ANN & ANFIS[22]) and artificial intelligence such as Genetic Algorithm (GA) [23], Particle Swarm Optimization (PSO) [24,25], and Teaching-learning-based optimization (TLBO) [26] techniques have been used to optimize the process parameters which influence tribological and machining behaviour of composites. However, it is observed that most of the results are not favourable due to the uncertainty associated with the process variables. Therefore, an attempt has been made in this work that optimization of tribological behaviour on the Al-CSAp composite using hybrid grey-fuzzy reasoning approach (GFRA). Three input parameters vis-a-vis load, % of CSAp and sliding distance are considered to study the responses such as wear rate, wear, and coefficient of friction.

2. EQUIPMENT AND TECHNIQUES

2.1 Materials and Preparation

In this study, aluminium (Table 1) was used as matrix and coconut shell ash was used as reinforcement. The aluminium coconut shell ash particulate composites (Al-CSAp-MMCs) were fabricated by using stir casting technique at 5, 10 and 15 % by volume.

Table 1. Composition of Al- Si-Fe.

Fe	Si	Cu	Zn	Mn	Residual	Bal
0.75 %	0.95 %	0.15 %	0.1 %	0.05 %	0.15 %	Al

2.2 Preparation of Coconut shell Ash Reinforcement Particles (CSAp)

In this work, CSAp has been prepared by crushing the coconut shells in a jaw crusher to get small flakes and then these flakes were crushed in a hammer mill to produce coconut shell pieces/particles. The obtained particles were filled into a Gr crucible and placed in a

tubular electric furnace at 1420 °C with argon atmosphere. Finally, the CSA was classified using sieve of mesh size ≤ 240 BSS (63 μm) vibrated with rotary sieve shaker. The particles passing through the sieve were collected in a pan and used as reinforcement in Al-Si-Fe for producing Al-CSAp composites. The CSA particles have been examined by X-ray diffraction (XRD) (Philips PW-1729) to know phases and chemical elements that are present by X-ray fluorescence (XRF) (SPECTRO) as shown in Table 2. Similarly, the density of particles was determined by pycnometer method and size of particles by laser scattering technique (Malvern Master 2000).

2.3 Preparation of Al-CSAp Composite

The compo casting technique was used for preparation of Al-CSAp MMCs. In this process, the aluminium matrix (Al-Si-Fe) was pre-heated at 450 °C and the heating was continued until Al-Si-Fe melted at 660 °C. The CSA particles were pre-heated in an electric arc furnace at 900 °C for 3 hours and charged into the crucible that contains semi-solid melt at a temperature of 645 °C. This enhanced retention and distribution of particles uniformly in the matrix. Thereafter, the molten metal and CSAp were stirred with PID controlled motor in the presence of argon gas at a speed of 600 RPM for 9 minutes to achieve homogeneous distribution of reinforced particles. The impeller had four blades made up of stainless steel material. To avoid reaction among aluminium and stirrer material at higher temperature, the stirrer was coated with zirconia. The main purpose of supplying argon gas is to evade the oxidation. Then, the melt was superheated above the liquid temperature at 690 °C and poured into a preheated (300 °C) cast iron mould of the size of 100×20×40 mm to obtain an Al-CSAp composite.

Table 2. Chemical Composition of CSA.

Constituents	wt.%
Fixed C	04-06
SiO_2	36-40
Fe_2O_3	08-09
Al_2O_3	23-25
MgO	02-03
CaO	03-05
K_2O	0.7 - 0.95

2.4 Hardness and Tensile Tests

For Al-CSAp MMCs, hardness test using Vickers hardness tester (Model: DHV 1000) has been performed with an applied load of 100 gm (0.98 N). On each specimen, five indentations have been made, and an average hardness number of the examined sample has been considered. The tensile properties of the developed composites (Al-CSAp) have been tested with Hounsfield tensometer (Model: ETM-ER3/772/12) at a cross head speed of 1 mm/sec with a maximum load of 20 kN, as shown in Fig. 1a. The tensile samples were prepared as per ASTM–E8.

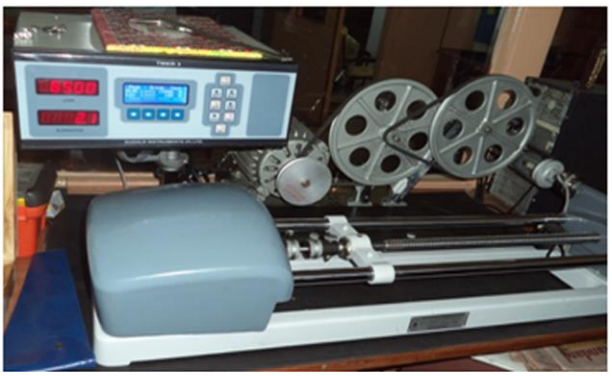

a)

b)

Fig. 1. Schematic picture of (a) Tensometer, (b) Pin-on-disc setup.

2.5 Optical Microscopic Studies

The Microstructural analysis has been conducted on the developed Al-CSAp composites. Samples were cut from the center of cast, polished in accordance with ASTM E-3 and finely etched with Keller's testing agent (ASTM-E 407). Afterward, the samples were inspected using microscope with image process analyzer (Infinity Lite, Model No: XJL-17).

Table 3. Parameters and their levels.

Control parameters	Symbol	Level		
		-1	0	1
Load, (N)	L	10	30	50
% of CSAp, (% of vol.)	R	5	10	15
Sliding distance, (m)	D	1000	2000	3000

2.6 Wear Test

Wear-tester (Fig. 1b; Model: DUCOM TR-201LE-PHM-400) has been used for examining wear resistance properties of Al-CSAp composites. The test samples were prepared as per ASTM G99-95 standards, having dimensions ø8 mm with 35 mm long. The tested specimens were slide against the steel disc (material EN-31), having hardness RC 62 with a surface roughness of 0.1 (R_a). Before testing, each specimen was polished with silica carbide emery paper of grits 240 follow-ups to 600 grits. Moreover, the experiments were conducted at a constant track of 50 mm diameter. The test samples were cleaned with acetone and measured their weight, by weight loss method using an electronic balance of accuracy 0.001 g. The difference in weights before and after wear of the sample was considered as weight loss. Wear was a linear dimensional loss of material over a sliding distance. Wear of material has recorded using linear variable differential transformer (LVDT) with measurable unit is μm [27]. The weight loss has been converted in to volume loss. Wear rate has signified the loss of material with specified time of abrasion. The ratio of volume loss to sliding distance is known as wear rate. The unit of wear rate is mm^3/m [17,28]. Coefficient of friction (COF) has also been calculated from frictional forces per unit normal load, for better results mean of the COF has been considered. The worn-out surfaces of composite were examined by SEM (Model no: JEOL JSM-5600LV). The results are depicted in Section 4 (Results and Discussion).

2.7 Experimental Design

The experiments are intended based on Taguchi's (L_{27}) orthogonal array. The experimental design comprises three factors such as load, % of CSAp and sliding distance and their levels as shown in Table 3. In Taguchi L_{27} design, the column 1st and 2nd was assigned to the load and % of CSAp respectively. To avoid overlapping and aliasing of interactions with columns factors, 3rd column was modified to the 5th column for a parameter, sliding distance. Therefore, 3rd and 4th columns have been allocated to the relations of the load and %of CSAp i.e. (L x R). Similarly, 6th and 7th columns have been assigned to the relations of load and sliding distance (L x D). The columns 8th and 11th are consigned for the interaction of % of CSAp and sliding distance (R x D). Remaining residual columns are assigned to error conditions [14,16,29]. Therefore, the designed Taguchi orthogonal array decides to select the runs in random order and to complete in the three consecutive repetitions for the experimental runs. Moreover, three responses such as wear, wear rate, and coefficient of friction were computed base on the L_{27} design. The results are shown in Table 4. The responses are described as quality attributes.

Table 4. Experimental results of Taguchi (L_{27}).

Run	L	R	D	Wear(μm)	Wear rate $*10^{-3}$	Coefficient of friction
1	10	5	1000	191	5.556	0.298
2	10	5	2000	193	2.815	0.188
3	10	5	3000	385	2.173	0.168
4	10	10	1000	185	5.000	0.285
5	10	10	2000	180	2.423	0.175
6	10	10	3000	210	2.159	0.148
7	10	15	1000	165	3.462	0.234
8	10	15	2000	175	2.327	0.165
9	10	15	3000	268	1.936	0.372
10	30	5	1000	380	6.333	0.415
11	30	5	2000	391	3.222	0.354
12	30	5	3000	478	2.704	0.293
13	30	10	1000	310	6.500	0.385
14	30	10	2000	285	3.115	0.325
15	30	10	3000	460	2.436	0.275
16	30	15	1000	268	5.808	0.372
17	30	15	2000	312	3.115	0.309
18	30	15	3000	426	2.321	0.225
19	50	5	1000	480	7.111	0.641
20	50	5	2000	521	4.167	0.485
21	50	5	3000	685	4.012	0.395
22	50	10	1000	415	6.923	0.636
23	50	10	2000	505	3.962	0.4565
24	50	10	3000	525	2.846	0.392
25	50	15	1000	398	6.615	0.62
26	50	15	2000	468	3.654	0.444
27	50	15	3000	478	2.641	0.378

Usually, Taguchi method is used to optimize the single response only; it cannot optimize multiple responses effectively. Therefore, it is necessary to convert multiple responses into equivalent single response for the successful implementation of the Taguchi approach to achieve best optimal parameter setting. Due to this reason, grey relational analysis has been used to convert

multiple responses into a single response. Grey theory also handles the uncertainty as well as vagueness in the physical variability of the input data. However, to validate the consistency of the obtained results, it is necessary to test for fuzzy logic approach. Therefore, the fuzzy logic concept has also been incorporated into handling the uncertainty involved in the process parameters. Hence, the obtained results were compared with grey relational grades to confirm the optimal performance.

2.8 Grey Relational Analysis (GRA)

The GRA is a technique which is used for handling the uncertainty of multiple variables and discrete data [36]. The procedural sequences of GRA are as follow:

Step-1:

The responses have been initially pre-processing the data by normalization to reduce inconsistency. The normalized values are used to transfer original to comparable sequence. These results should vary in between {0, 1}. If the value of target is infinite at original progression, then the original sequence of characteristic followed by the higher-is-better; smaller-the-better and definite value of target (desired value) criteria [19,21,30].

When smaller-is-the-better, original sequence could be normalised as follows:

$$X_k(n) = \left(\frac{\max y_k(n) - y_k(n)}{\max y_k(n) - \min y_k(n)} \right) \quad (1)$$

Where, $(X_k(n))$ are the normalized grey relation values for the n^{th} response, $\max y_k(n)$ and $\min y_k(n)$ are the greatest and least values of $y_k(n)$ for n^{th} response. Experimental runs (k=1, 2 ...) and number of factors (n=1, 2 ... n).

Step-2:

Thereafter, determination of normalization to calculate the grey relational coefficient is as follows:

$$\xi_k(n) = \frac{(\Delta_{min} - \zeta\Delta_{max})}{(\Delta_{ok}(n) + \zeta\Delta_{max})} \quad (2)$$

Where $\Delta_{ok}(n)$ represents the deviation sequence from the reference sequence, which can be computed by the difference between $x_o(n)$ and $x_k(n)$ with absolute significance. Distinguishing coefficient (ζ) value is considered based on distinguished ability. Generally, the value of distinguishing coefficient (ζ) is taken as 0.5.

$$\Delta_{ok}(n) = \left\| x_o(n) - x_k(n) \right\| \quad (3)$$

Step-3:

The grey relational grades (GRG) can be calculated by the average of grey relational coefficients (GRC) for each objective of responses.

$$\gamma_k = \frac{1}{n} \sum_{k=1}^{n} \xi_k(n) \quad (4)$$

The GRG value indicates the overall performance index. Higher the value of GRG, the better is the performance.

2.9 Grey – Fuzzy Reasoning Analysis

Fuzzy logic deals with uncertainties and permits the assimilation of the options on making an appropriate decision. Moreover, fuzzy logic is a mathematical tool, utilized to handle the imprecision, uncertainty, and vagueness in the human judgment process [27,30-31]. The uncertainty due to physical variability of various input process parameters can be tackled by the fuzzy reasoning approach. Therefore, fuzzy logic mainly consists of three elements such as fuzzifier, inference engine with the knowledge base and defuzzifier. The main function of fuzzifier is to convert the inputs towards a crisp form which contain specific information about the linguistic variables. In addition, fuzzifier uses input data onto inexact query and expresses in fuzzy variables based on the membership function. The fuzzy membership grade lies in between {0, 1}. Fuzzy inference system contains two types of knowledge bases which are Mamdani and Sugeno. The knowledge base contains rule and database. The database refers the number of membership functions handling fuzzy set while rule base includes logical operations like IF-THEN laws. The inference scheme to perform interference with operations based on the rules. Defuzzifier provides the required productivity from the fuzzy system in the form of firm data. The method of

defuzzification uses the center of area (COA) technique to calculate the firm output. The fuzzy logic approach must provide the better performance due to the minimum vague output than the GRG apart [21,30] . Therefore, fuzzy logic combined with GRA to obtain the grey fuzzy reasoning grade (GFRG) and that must be more than GRG [21,30,32–34].

3. RESULTS AND DISCUSSION

3.1 Mechanical properties of Al-CSAp MMC

XRD profile (Fig. 2) reveals that coconut shell ash contains crystalline phase elements with variation in peak intensity. XRF revealed chemical compositions of CSA which are shown in Table 2. SiO_2 (Silicon oxide), Al_2O_3 (Aluminium oxide) and Fe_2O_3 (Ferric Oxide) are the major and MgO (Magnesium oxide) CaO (Calcium oxide) and K_2O(Potassium oxide) are minor constituents of the CSA. The oxides like SiO_2, Al_2O_3 and Fe_2O_3 make the matrix harder and more durable which results in improved physical-mechanical properties. Al_2O_3 and SiO_2 are well-known reinforcing additives for improving wear resistance and strength for Al-MMCs. CaO could react with alumina and silica to form aluminates and calcium silicates, which have good adhesive properties and improve to load bearing capability of the composites [35]. MgO is a refractory material, which can withstand high temperature and has a low thermal conductivity [36]. The XRD peaks show the existence of carbon, apparently in the outward appearance of graphite.

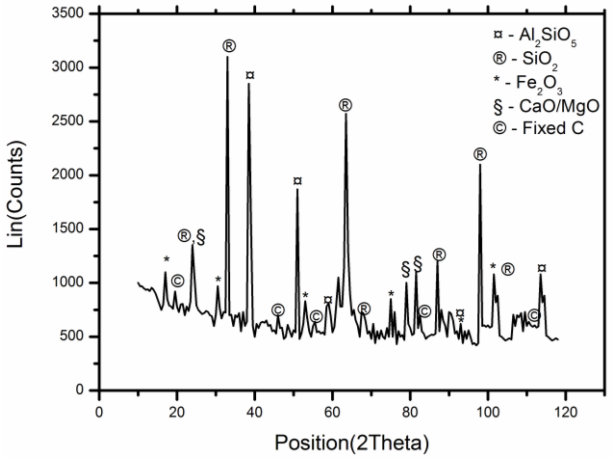

Fig. 2. XRD of Coconut Shell Ash.

Figure 3 shows the reinforcing particles of CSA and shape respectively. From Fig. 3, the reinforcing particle (CSA) has been seen to have spherical shape; an average size of 42 μm with a density 2.04 g/cm^3.

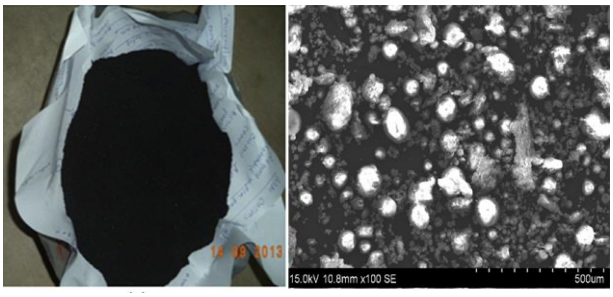

Fig. 3. SEM of CSA particulates.

The hardness of Al-CSAp composites increased due to the hard phase of CSA particle in addition to the homogeneous distribution of CSAp within the Al-Si-Fe matrix. Composite properties were enhanced due to the presence of alkali earth metal such as CaO and MgO in CSA. Elemental analysis of a composite was examined with SEM-EDX, shown in Fig. 4. The tensile strength increased with increases in volume fraction of CSA particle. Moreover, a decrease in elongation was noticed with the addition of CSA particles. The hardness of composite increased by 6.08, 26.62 and 29.87 % at 5, 10, 15 % of CSA additions, respectively as compared to unreinforced metal (Al-Si-Fe).

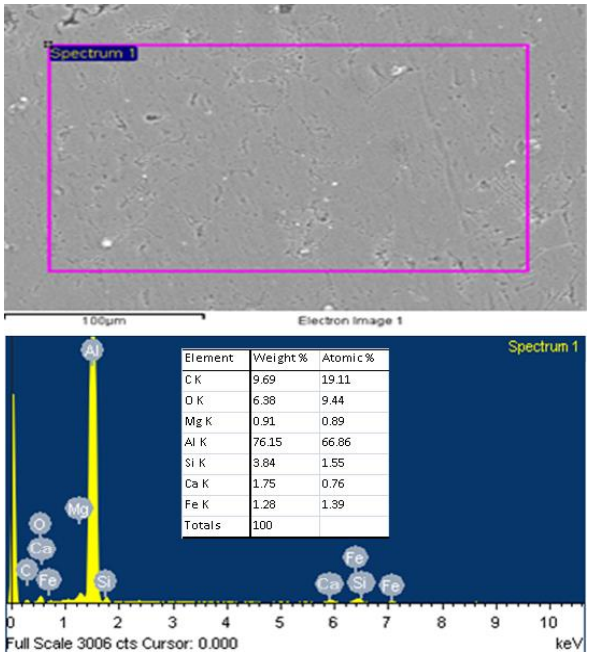

Fig. 4. Elemental analysis of Al-CSA composite.

Tensile strength and percentage elongation are directly and indirect proportional characters to the reinforcement. The properties of composites are enhanced due to strain hardening of the composite as observed in Table 5. Moreover, with the addition of reinforcement, tensile strength significantly increased from 91 Nmm^{-2} of unreinforced Al-Si-Fe to 143 Nmm^{-2} at 15 % CSA additions. Similarly, density of composite decreased by 1.85, 3.69, and 5.90 % at 5, 10, and 15 % of CSA, respectively as compared to Al-Si-Fe. Reinforcement particles are hard phase protrusions which absolutely prevent the matrix from surface abrasion due to cutting action of the disc. Moreover, it increases the load bearing capability, constraints dislocation movement, reduces inter planar pacing and makes the dislocation movement critical.

Table 5. Mechanical Properties of Al-CSA-MMCs.

Composite	HV	Density	UTS	% of Elongation.
		(g/cm^3)	(N/mm^2)	(mm)
Al-Si-Fe	58.26	2.71	91	29.7
Al-5%CSA	62.03	2.66	102	23.3
Al-10%CSA	79.4	2.61	127	18.3
Al-15%CSA	83.07	2.55	143	16

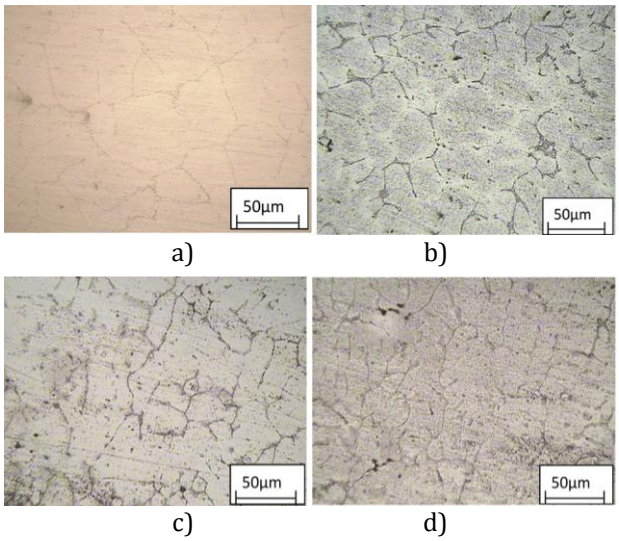

Fig. 5. Microstructure of (a) Al-Si-Fe (b) Al-5 % of CSA (c) Al-10 % of CSA (d) Al-15 % of CSA.

3.2 Metallographic and Surface Morphology

The microstructures of the pure and reinforced MMCs are presented in Fig. 5. The metallography images observed are bright area specifying the matrix and the dark area specifying reinforcement particles. The distribution of particles in the microstructure observed to be uniform. From Fig. 5a, it justifies equiaxed dendrite structure. Similarly, Fig. 5(b-d) revealed that addition of CSA to Al-alloy caused a grain refinement which could be responsible for enhancement in the tensile strength of the composite [37-38].

Table 6. The Grey relation coefficient and grey relational grade for quality attributes.

	GRG Coefficients				
Trails	Wear	Wear rate	Coefficient of friction	GRG	GRG Rank
ζ1	0.909	0.417	0.622	0.649	12
ζ2	0.903	0.746	0.86	0.837	4
ζ3	0.542	0.916	0.925	0.794	5
ζ4	0.929	0.458	0.643	0.676	9
ζ5	0.945	0.842	0.901	0.896	3
ζ6	0.852	0.912	1	0.921	2
ζ7	1	0.629	0.741	0.79	6
ζ8	0.963	0.869	0.935	0.922	1
ζ9	0.716	1	0.524	0.747	7
ζ10	0.547	0.37	0.48	0.466	22
ζ11	0.535	0.668	0.545	0.583	16
ζ12	0.454	0.771	0.63	0.618	14
ζ13	0.642	0.362	0.51	0.505	20
ζ14	0.684	0.687	0.582	0.651	11
ζ15	0.468	0.838	0.66	0.656	10
ζ16	0.716	0.401	0.524	0.547	18
ζ17	0.639	0.687	0.605	0.644	13
ζ18	0.499	0.871	0.762	0.711	8
ζ19	0.452	0.333	0.333	0.373	27
ζ20	0.422	0.537	0.422	0.461	24
ζ21	0.333	0.555	0.499	0.463	23
ζ22	0.51	0.342	0.336	0.396	26
ζ23	0.433	0.561	0.444	0.479	21
ζ24	0.419	0.74	0.503	0.554	17
ζ25	0.527	0.356	0.343	0.409	25
ζ26	0.462	0.601	0.454	0.506	19
ζ27	0.454	0.786	0.517	0.586	15

3.3 ANOVA of GRA

From the GRA, the quality attributes are normalised $(X_k(n))$ to maintain the consistency. The values are lied in between {0, 1}, followed by Eq. 1. Then, the GRC has been calculated using Eq. 2. Afterwards, the GRG is determined using Eq. 4. The obtained results of GRC and GRG have shown in Table 6. The GRG value indicates the overall performance index of individual experimental run. The experimental run eight indicates the highest GRG value, which represents best performance. The effects of each individual factor at every level are shown in Table 7. It revealed that the load (L) was the most influencing factor at level-1 (10 N) followed by sliding distance (D) at level-3(3000 m) and % of CSAp (R) at level-3 (15 %). The

highest average grey relational grade for each optimal parameter state for minimal quality attributes has been found as $L_1R_3D_3$.

Table 7. Response Table for GRG.

Level	L	R	D
1	0.8037	0.5825	0.5345
2	0.5976	0.6371	0.6642
3	0.4695	0.6512	0.6721
Delta	0.3342	0.0686	0.1376
Rank	1	3	2

ANOVA (Table 8) revealed that the load (73.90 %) was higher influencing parameter followed by sliding distance (17.74 %) and % of CSAp (3.73 %). The contributions of overall factors are performed 97.9 % of the total variance in GRG. Contributions of percentage are estimated through sum of square of deviation divided by the total mean of GRG.

Table 8. Analysis of Variance for GRG.

Source	DF	Seq SS	Adj SS	Adj MS	F - Value	Contri. (%)
L	2	99.54	99.54	49.77	142.67	73.9
R	2	5.03	5.03	2.51	7.21	3.73
D	2	23.90	23.90	11.95	34.26	17.74
L*R	4	0.35	0.35	0.09	0.25	0.26
L*D	4	2.27	2.27	0.57	1.62	1.68
R*D	4	0.82	0.82	0.21	0.59	0.61
Error	8	2.79	2.79	0.35		2.07
Total	26	134.70				100
S = 0.5906 R-Sq = 97.9 % R-Sq(adj) = 93.3 %						
DF: degree of freedom; SS: sum of squares; MS: Mean sum of squares ; Contri.: contribution						

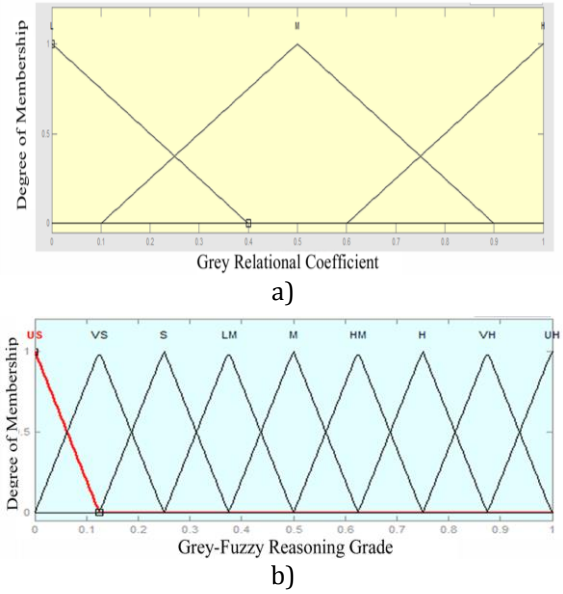

Fig. 6. Membership function and Fuzzy subset used for GFRG.

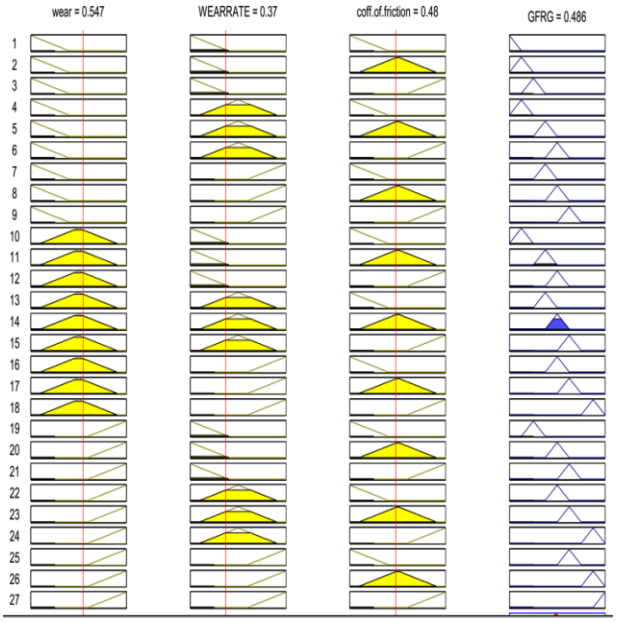

Fig. 7. Computation of GFRG for Experimental Run 10.

3.4 Grey – Fuzzy Reasoning Analysis (GFRA)

The three normalized quality attributes are used as inputs for fuzzy controller. Three fuzzy linguistic variables (Fig. 6a) are used as input variable and nine linguistic variables (Fig. 6b) are used as output by which 27 rules can be formed to attain the GFRG using MATLAB 7.0 software. The input variables are required to fuzzify using suitable linguistic ideals. Afterward, the defuzzification is executed by the COA method for estimating the firm value (output) as GFRG. The GFRG value for a particular experiment (Expt. No. 10) is shown in Fig. 7. Similarly, for all 27 experiments, the GFRG values are listed in Table 9.

Table 9. Grey fuzzy reasoning grade with ranks.

Run	GFRG	GFRG RANK	Run	GFRG	GFRG RANK
1	0.651	11	15	0.658	10
2	0.832	5	16	0.549	17
3	0.875	4	17	0.591	14
4	0.672	9	18	0.74	7
5	0.923	3	19	0.389	27
6	0.929	2	20	0.5	20
7	0.745	6	21	0.47	24
8	0.938	1	22	0.398	26
9	0.728	8	23	0.5	21
10	0.486	23	24	0.558	16
11	0.53	18	25	0.414	25
12	0.609	13	26	0.5	22
13	0.502	19	27	0.576	15
14	0.63	12			

On the comparison of grey relational grade (GRG) presented in Table 6 with grey-fuzzy reasoning grade (GFRG) (Table 9), it is observed that GFRG values are improved which reduces the uncertainty of statistical values. From the main effect plot (Fig. 8), it can be observed that the GFRG are high at the level of L_1 (Load-10 N), R_3 (% of CSAp -15 %) and D_3 (Sliding Distance - 3000 m). From the statistical analysis, the input variable combination ($L_1R_3D_2$) such as load of 10 N, % of CSAp of 15 and sliding distance 2000 m produced the highest GFRG value of 0.938. It is closer to the reference value of '1'. This reflects the significant effect on GFRG. The GRG and GFRG values for all the experimental design is shown in Fig. 9. ANOVA of GFRG (Table 10) revealed that the load (72.83 %) was the highest influencing parameter followed by sliding distance (18.36 %) and % of CSAp (2.21 %). The contributions of overall factors are obtained 96.68 % of the total variance in GFRG.

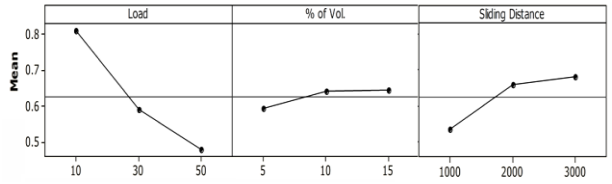

Fig. 8. Response graph for GFRG value.

Table 10. Analysis of Variance for GFRG.

Source	DF	Seq SS	Adj SS	Adj MS	F – Value	Contri. (%)
L	2	95.71	95.71	47.85	87.69	72.83
R	2	2.91	2.91	1.45	2.67	2.21
D	2	24.12	24.12	12.06	22.1	18.36
L*R	4	0.89	0.89	0.22	0.41	0.68
L* D	4	2.6	2.6	0.65	1.19	1.98
R* D	4	0.82	0.82	0.2	0.37	0.62
Error	8	4.37	4.37	0.55		3.32
Total	26	131.42				100
S = 0.7387 R-Sq = 96.7 % R-Sq(adj) = 89.2 %						

3.5 Effect of Responses and Wear Behavioural Parameters on GFRG

The dissimilarity of wear behavioural limits of response on GFRG is illustrated in Figs. 10 and 11, respectively. It revealed that, Fig 11 showed GFRG values at various interaction levels which were high at L_1R_2, L_1D_3, and R_3D_1, whereas a minimum was achieved at L_3R_1, L_3D_1, and R_1D_3. Figure 11a shows that while % of CSAp increases GFRG increases with decreasing load. At the condition of 10 % CSAp and load 10 N, the GFRG value is high (0.923), at inferior load and higher volume fraction of Al-CSA composites has resistance to dislocation movement of slipping planes (plastic deformation) due to harder phase reinforced particulates (CSA). Moreover, this increases the yield strength with distinct barrier possibly pitched obstruent of dislocation [1,39-40]. Therefore, GFRG increases with increase in reinforcement which prevents the movement of dislocations. The hardness of composites has been increases with increase of CSA. Similarly, the GFRG value is least (0.389) at the condition of 5 % of CSAp (lowest reinforcement) and maximum load (50 N).

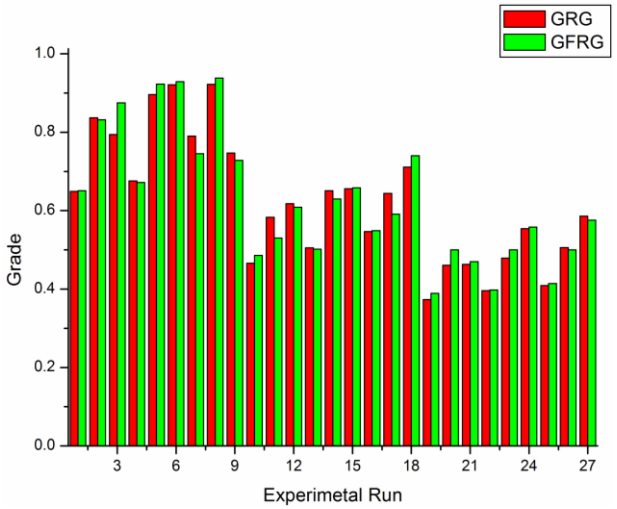

Fig. 9. Evaluation of grey relational grade and grey-fuzzy reasoning grade.

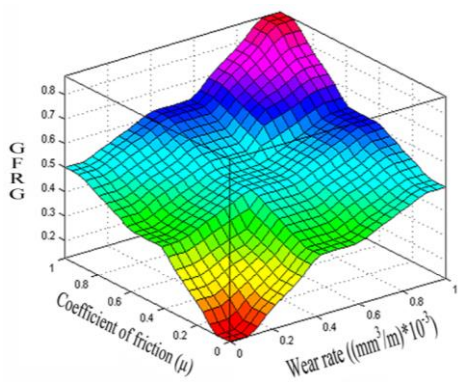

Fig. 10. Variation of Grey-fuzzy Reasoning Analysis (GFRA) on GRC of response.

From Fig. 11b, it is observed that at a constant sliding speed, the GFRG value is inversely proportional to the load and directly proportional to sliding distance. Generally, Wear is directly proportional to applied load. The matrix has become harder due to the addition of reinforced particles (CSA), thus prevents direct metal- metal contact. The reinforced particles (CSA) lie between tribo surfaces (i.e. pin and disc), reduces

coefficient of friction. Due to hardness of composite, wearing of steel disc occurs hence to form a layer (oxide) on counter face due to the transfer of iron oxide particles from disc to pin. Similarly, while sliding a mechanically mixed layer (MML) appears at the steel disc due to the presence of graphite in the form of crystal; this enhances the wear resistance of composite. However, while neither increasing speed nor sliding distance, the reinforcement particles were come out from the matrix. The harder particles were laid on contact surface and reduced frictional forces between tribo-surfaces. Even if load increase the particles were wrecked and the protective layer (i.e. oxide layer and MML) among tribo-surfaces also diminished in a shorter interval of time [10,41,42]. Hence, wear rate and coefficient of friction has increased.

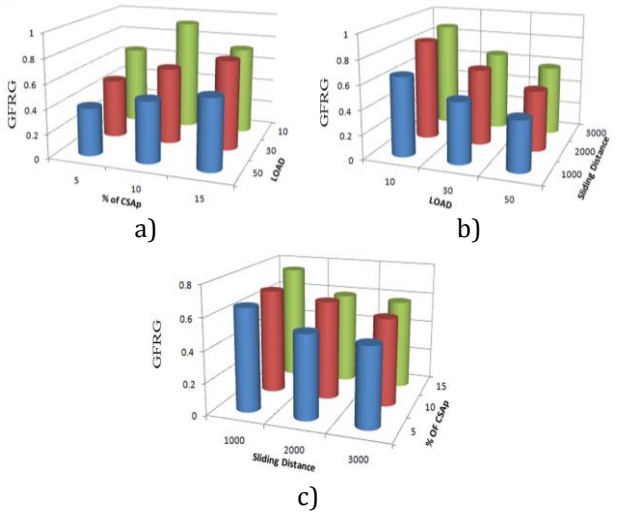

Fig. 11. Effect of Grey -Fuzzy Grade (GFRG) on wear behavioural parameters (a) load vs. % of CSAp on GFRG (b) Sliding distance vs. Load on GFRG (c) % of CSAp vs. sliding distance on GFRG.

The GFRG value is high (0.875) at the condition of least load (10 N) and highest sliding distance (3000 m). Similarly, at maximum load of 50 N and least sliding distance of 1000 m, the value of GFRG is small (0.414). The combined effect of sliding distance and the volume percent of reinforcement effect on GFRG is shown in Fig. 11c. At constant percentage of reinforcement, the sliding distance increases with decreases of GFRG. GFRG value is high (0.745) at 15 % volume of CSAp with a sliding distance of 1000 m whereas GFRG is low (0.5) at 5 % of CSAp and sliding distance of 3000 m. The GFRG is increased with increase of reinforcement (CSAp) which enhances the strength of the developed MMC. At an inferior coefficient of friction, the composite may be attributing to form a thin film between tribo surfaces, performing like self-protective layer.

Table 11. Results of wear behaviour performance with initial and optimal setting of parameters.

PC	$L_1R_1D_1$	$L_1R_3D_3$	Gain	Imp. (%)	Error
GFRG exp.	0.651	0.728	0.077	10.58	0.156
GFRG pre.		0.884	0.233	26.35	
GRG exp.	0.649	0.747	0.098	13.09	0.133
GRG Pre.		0.88	0.231	26.23	
Wear	191	268	77	28.73	
Wear Rate	5.556	1.936	-3.62	65.16	
Coeff.	0.298	0.372	0.074	19.89	
PC - Performance characteristics; exp. - experimental; Pre. - Predicted; Coeff. - Coefficient of friction; Imp. – Improvement					

4. CONFIRMATION TEST:

The predicted GFRG (η) at optimal rank of factors is considered by Eq. 5.

$$\eta_{predicted} = \eta_m + \sum_{k=1}^{n}(\bar{\eta}_k - \eta_m) \qquad (5)$$

Whereas η_m is the mean of GRG of all the experimental runs, $\bar{\eta}_k$ is the mean of optimal value of k^{th} experiment, and n is the number of index factors.

The experiment number one is considered as the initial conditional parameters ($L_1R_1D_1$) which can be observed in Table 4. The results of confirmation test shown in Table 11 that specifies the initial parameters of GFRG value is 0.651 and an optimal parameter of predicted GFRG is 0.884. The wear is increased from 191 to 268 μm and wear rate is reduced from 5.556 to 1.936. Consequently, the coefficient of friction is improved from 0.298 to 0.372. Therefore, wear resistance and coefficient of friction were improved by 28.73 % and 19.89 %, respectively. In addition, wear rate is reduced by 65.16 %. Thus, GFRG in wear behavioural parameters of CSAp composites has better improvement (0.233) by using grey-fuzzy reasoning approach (GFRA) and error is less than ±5, which is significant.

In this section, a comparative study of prepared CSA composites with pure alloy is analyzed. The

scanning electron microscope (SEM) photographs of unreinforced alloy and CSA composites are tested under the condition of constant load (30 N) and sliding distance (2000 m) with velocity (1.5 m/s).

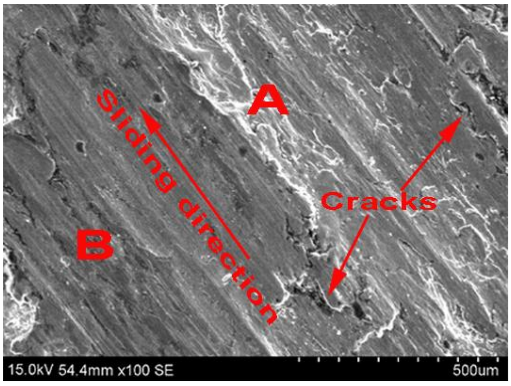

a)

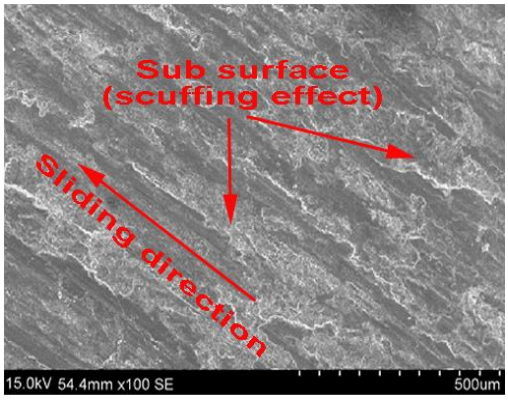

b)

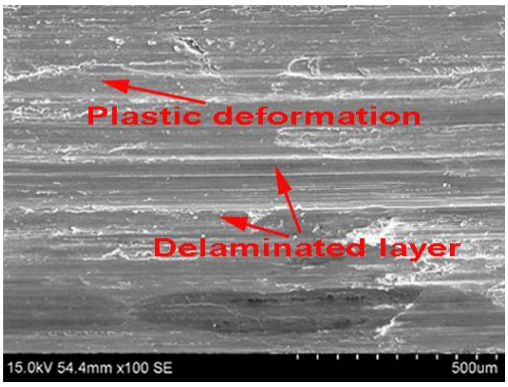

c)

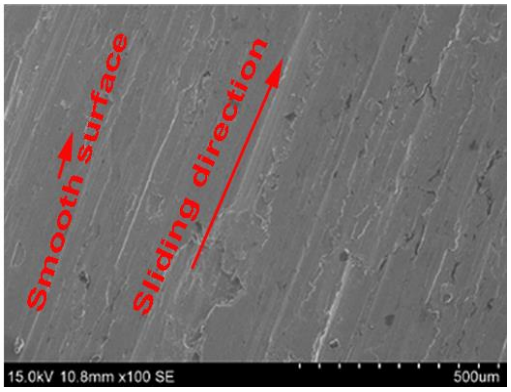

d)

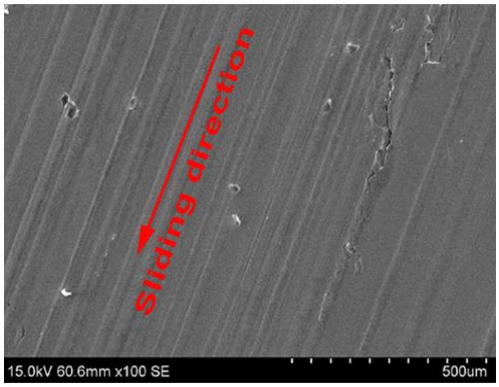

e)

Fig. 12. SEM worn-out surfaces (a) pure (b) Al-5 % of CSA (c) Al-10 % of CSA (d) Al-15 % of CSA (e) optimal condition.

From Fig. 12, it can be observed that the particle pull-outs, micro cutting, deep penetration (groove) formation and fracture surfaces are present in the composite worn-out surface. Thus, it confirms the wear mechanism has occurred between pin and counter face. Figure 12a (SEM of unreinforced alloy) shows the worn-out surface in the form of wider grooves, deep cuttings and some micro cracks that can be observed in the region parallel to the sliding direction. Moreover, two different kinds of wear region observed in unreinforced alloy i.e. adhesion (A) and abrasion (B). The coefficient of friction is high at beginning, hence the movement between pin and disc becomes difficult. However, temperature is raised in the base matrix due to high frictional forces which cause softening of the material and leads to plastic deformation. This affects wear loss. The wear loss increases due to the loss of material. It can be viewed in the form of debris. The cracks are formed due to the deep recess effect exerted by the hardened debris of the matrix.

Similarly, Figs. 12b-d show the SEM of the 5 %, 10 %, and 15 % worn out surface of CSAp reinforced Al-MMCs. Moreover, it is confirmed that as the % of reinforcement increases, the composite become thermally stable and its hardness is improved due to plastic deformation. Due to this reason only, the composites could withstand the effect of wear rate. The composite is tested under the condition of optimal setting ($L_1R_3D_3$) which can be understood from the worn-out surface shown in Fig. 12e. From the morphology, the grooves are very fine and the plastic deformation at the edge of grooves is less. So, at the above optimal condition, the material withstood the effect of friction and wear.

5. CONCLUSIONS

In this paper, the CSAp reinforced aluminium composites were developed by compo casting technique at 5, 10 and 15 % by volume. The tensile strength and hardness both increase with increases of % of CSAp whereas % elongations and density decreases. The wear behaviour of composite is analysed considering three quality attributes with three input process parameters such as load, % of CSAp and sliding distance. The wear behavioural parameters are optimized with respect to the grey relational grade to accomplish the reduction of wear and weight loss due to friction and improves wear rate. Here, a hybrid (Grey-fuzzy) optimization technique has been adopted to find the optimal levels of input parameters by using Taguchi's orthogonal array (L_{27}). From the statistical analysis, the input parameter combination ($L_1R_3D_2$) such as the load of 10 N, % of CSAp of 15 and sliding distance 2000 m provides a highest GFRG value of 0.938. It is closer to the value of reference '1'. This reflects the significant effect on GFRG. From the ANOVA test, the optimal condition obtained ($L_1R_3D_3$) which indicates the load of 10 N, % of CSAp of 15 and sliding distance 3000 m. The load (72.83 %) is the highest influencing parameter followed by sliding distance (18.36 %) and % of CSAp (2.21 %). The contributions of overall factors are performed 96.68 % of the total variance in GFRG. From the GFRG optimal condition, the wear is increased from 191 to 268 μm, wear rate is reduced from 5.556 to 1.936 and coefficient of friction is improved from 0.298 to 0.372 respectively.

REFERENCES

[1] M.K. Surappa, 'Aluminium matrix composites: Challenges and opportunities', *Sadhana*, vol. 28, no. 1&2, pp. 319–334, 2003.

[2] C. Zweben, 'Metal-matrix composites for electronic packaging', *JOM*, vol. 44, no. 7, pp. 15–23, 1992.

[3] M.I. Pech-Canul, 'Aluminum Alloys for Al/SiC Composites', in *Recent Trends in Processing and Degradation of Aluminum Alloys*, Z. Ahmad, Ed. InTech, 2011, pp. 299–314.

[4] P.K. Rohatgi, 'Metal-matrix Composites', *Defence Science journal*, vol. 43, no. 4, pp. 323–349, 1993.

[5] D.B. Miracle, 'Metal matrix composites – From science to technological significance', *Composites Science and Technology*, vol. 65, pp. 2526–2540, 2005.

[6] R. Siva Sankara Raju, M.K. Panigrahi, R.I. Ganguly and G. Srinivasa Rao, 'Investigation of Tribological Behavior of a Novel Hybrid Composite Prepared with Al-Coconut Shell Ash Mixed with Graphite', *Metallurgical and Materials Transactions A*, vol. 48, no. 8, pp. 3892–3903, 2017.

[7] J.A. Youngquist, B.E. English, R.C. Scharmer, P. Chow and S. R. Shook, 'Literature review on use of nonwood plant fibers for building materials and panels', *Gen. Tech. Rep. FPL-GTR-80. Madison, WI: U.S. Department of Agriculture, Forest Service, Forest Products Laboratory*, pp. 26–188, 1994.

[8] Y. Sahin, 'Wear behaviour of aluminium alloy and its composites reinforced by SiC particles using statistical analysis', *Materials and Design*, vol. 24, no. 2, pp. 95–103, 2003.

[9] M. Kök and K. Özdin, 'Wear resistance of aluminium alloy and its composites reinforced by Al_2O_3 particles', *Journal of Materials Processing Technology*, vol. 183, no. 2–3, pp. 301–309, 2007.

[10] A. Baradeswaran, S.C. Vettivel, A. Elaya Perumal, N. Selvakumar and R. Franklin Issac, 'Experimental investigation on mechanical behaviour, modelling and optimization of wear parameters of B_4C and graphite reinforced aluminium hybrid composites', *Materials and Design*, vol. 63, pp. 620–632, 2014.

[11] J. Babu Rao, D. Venkata Rao, K. Siva Prasad, N. R.M.R. Bhargava, 'Dry sliding wear behaviour of fly ash particles reinforced AA 2024 composites', *Materials Science-Poland*, vol. 30, no. 3, pp. 204–211, 2012.

[12] S.B. Venkata Siva, R.I. Ganguly, G. Srinivasa Rao and K.L. Sahoo,'Wear behaviour of novel Al based composite reinforced with ceramic composite (Al_2O_3–SiC–C) developed from colliery shale material', *Tribology - Materials, Surfaces & Interfaces*, vol. 8, no. 3, pp. 117–124, 2014.

[13] S.Y. Aku, D.S. Yawas and A. Apasi, 'Evaluation of Cast Al-Si-Fe alloy / Coconut Shell Ash Particulate Composites', *Gazi University Journal of Science*, vol. 26, no. 3, pp. 449–457, 2013.

[14] R. Siriyala, G. krishna Alluru, R. Penmetsa and M. Duraiselvam,'Application of grey-taguchi method for optimization of dry sliding wear properties of aluminum MMCs', *Frontiers of Mechanical Engineering*, vol. 7, no. 3, pp. 279–287, 2012.

[15] A. Bendell, J. Disney and W.A. Pridmore, 'Reviewed Work: Taguchi Methods: Applications in World Industry', *Interfaces (Providence)*, vol. 21, no. 2, pp. 99–101, 1991.

[16] G. Taguchi, 'Introduction to quality engineering: designing quality into products and processes', in *Vol. 4*, 2nd ed., Tokyo: Asian Productivity Organization., 1986, p. 191.

[17] N. Radhika, 'Fabrication of LM25 / SiO_2 Metal Matrix Composite and Optimization of Wear Process Parameters Using Design of Experiment', *Tribology in industry*, vol. 39, no. 1, pp. 1–8, 2017.

[18] S.R. Chauhan and K. Dass, 'Dry Sliding Wear Behaviour of Titanium (Grade 5) Alloy by Using Response Surface Methodology', *Advances in Tribology*, vol. Article ID, p. 9 pages, 2013.

[19] J. Sudeepan, K. Kumar, T.K. Barman and P. Sahoo, 'Mechanical and Tribological Behavior of ABS/TiO_2 Polymer Composites and Optimization of Tribological Properties Using Grey Relational Analysis', *Journal of The Institution of Engineers (India): Series C*, vol. 97, no. 1, pp. 41–53, 2015.

[20] T. Rajmohan, K. Palanikumar and M. Kathirvel, 'Optimization of machining parameters in drilling hybrid aluminium metal matrix composites', *Transactions of Nonferrous Metals Society of China*, vol. 22, pp. 1286–1297, 2012.

[21] D. Julong, 'Introduction to Grey System Theory', *The Journal of Grey System*, vol. 1, pp. 1–24, 1989.

[22] H. Alimam, M. Hinnawi, P. Pradhan and Y. Alkassar, 'ANN & ANFIS Models for Prediction of Abrasive Wear of 3105 Aluminium Alloy with Polyurethane Coating,' *Tribology in industry*, vol. 38, no. 2, pp. 221–228, 2016.

[23] G. Cheng and Y. Xiaoyong, 'A Programming of Genetic Algorithm in Matlab7.0', *Modern applied science*, vol. 5, no. 1, pp. 230–235, 2011.

[24] S. Bharathi Raja and N. Baskar, 'Expert Systems with Applications Application of Particle Swarm Optimization technique for achieving desired milled surface roughness in minimum machining time', *Expert Systems With Applications*, vol. 39, no. 5, pp. 5982–5989, 2012.

[25] M. Azadi and M. Farhad, 'Application of orthogonal array technique and particle swarm optimization approach in surface roughness modification when face milling AISI1045 steel parts, '*Journal of Industrial Engineering International*, vol. 12, no. 2, pp 199–209 2015.

[26] R. Venkata Rao and V. Patel, 'An improved teaching-learning-based optimization algorithm for solving unconstrained optimization problems', *Scientia Iranica*, vol. 20, no. 3, pp. 710–720, 2013.

[27] A. Mukhopadhyay, S. Duari, T. K. Barman and P. Sahoo, 'Evaluation of Tribological Properties and Optimization of Electroless Ni-P-W Coating under Dry Condition using Grey Fuzzy Analysis,' *Tribology in Industry*, vol. 39, no. 1, pp. 50–62, 2017.

[28] N. Radhika, A. Vaishnavi and G.K. Chandran, 'Optimisation of dry sliding wear process parameters for aluminium hybrid metal matrix composites,' *Tribology in Industry*, vol. 36, no. 2, pp. 188–194, 2014.

[29] T. Bement, 'Taguchi Techniques for Quality Engineering', *Technometrics*, vol. 31, no. 2, pp. 253–255, 1989.

[30] T. Rajmohan, K. Palanikumar and S. Prakash, 'Grey-fuzzy algorithm to optimise machining parameters in drilling of hybrid metal matrix composites', *Composites Part B*, vol. 50, pp. 297–308, 2013.

[31] L.A. Zadeh, 'Fuzzy Sets', *Information and Control*, vol. 8, pp. 338–353, 1965.

[32] Y.S. Yang and W. Huang, 'A grey-fuzzy Taguchi approach for optimizing multi-objective properties of zirconium-containing diamond-like carbon coatings', *Expert Systems with Applications*, vol. 39, no. 1, pp. 743–750, 2012.

[33] A. Mukhopadhyay, S. Duari, T. K. Barman and P. Sahoo, 'Tribological Performance Optimization of Electroless Ni–B Coating under Lubricated Condition using Hybrid Grey Fuzzy Logic,' *Journal of The Institution of Engineers (India): Series D*, vol. 97, no 2, pp 215–231, 2016.

[34] T.J. Ross, '*Fuzzy Logic with Engineering Applications*', 2nd ed. John Wiley & Sons Ltd, 2004.

[35] M. Kenny and T. Oates, 'Lime and Limestone', in *Ullmann's Encyclopedia of Industrial Chemistry*, Weinheim, Germany: Wiley-VCH Verlag GmbH & Co. KGaA, 2007.

[36] M.A. Baghchesara, H. Abdizadeh and H.R. Baharvandi, 'Effects of MgO Nano Particles on Microstructural and Mechanical Properties of Aluminum Matrix Composite Prepared via Powder Metallurgy Route', *International Journal of Modern Physics: Conference Series*, vol. 5, pp. 607–614, 2012.

[37] S.A. Bello, I.A. Raheem and N.K. Raji, 'Study of tensile properties, fractography and morphology of aluminium (1xxx)/coconut shell micro particle composites,' *Journal of*

King Saud University - Engineering Sciences, vol. 29, no. 3, pp. 269-277, 2017.

[38] S.B. Hassan and V.S. Aigbodion, 'Effects of eggshell on the microstructures and properties of Al–Cu–Mg/eggshell particulate composites', *Journal of King Saud University - Engineering Sciences*, vol. 27, no. 1, pp. 49–56, 2015.

[39] J.A. Williams, 'Wear and wear particles — some fundamentals', *Tribology International*, vol. 38, pp. 863–870, 2005.

[40] K. Kato, 'Wear in relation to friction — a review', *Wear*, vol. 241, pp. 151–157, 2000.

[41] R.N. Rao and S. Das, 'Effect of applied pressure on the tribological behaviour of SiCp reinforced AA2024 alloy', *Tribiology International*, vol. 44, no. 4, pp. 454–462, 2011.

[42] E.A. Diler and R. Ipek, 'Main and interaction effects of matrix particle size , reinforcement particle size and volume fraction on wear characteristics of Al – SiCp composites using central composite design', *Composites: Part B*, vol. 50, pp. 371–380, 2013.